



# An Application of Rock Engineering System for Assessment of the Rock Mass Fragmentation: A Hybrid Approach and Case Study

Amir Azadmehr<sup>1</sup> · Seyed Mohammad Esmaeil Jalali<sup>1</sup> · Yashar Pourrahimian<sup>2</sup>

Received: 29 June 2018 / Accepted: 13 May 2019 / Published online: 18 June 2019  
© Springer-Verlag GmbH Austria, part of Springer Nature 2019

## Abstract

Rock mass fragmentation process plays a major role in the design of the block cave mining. To assess rock mass fragmentation, identification and determination of influencing parameters are crucial. In most case studies, the cross-impact or indirect interaction of influencing parameters has not been considered in the assessment of rock mass fragmentation. The aim of this paper is to present a hybrid approach to consider the direct and indirect effects of influencing parameters on rock mass fragmentation by use of classic rock engineering system (RES) and matrices impact cross multiplication applied to classification method (MICMAC). The most important effective parameters in the system were identified and ranked based on both RES and hybrid approach. Thereafter, the indirect fragmentation index was calculated for RENO and Diablo Regimete mines in Chile and Kemess mine in Canada. An appropriate consistency was found between the results of the hybrid approach and available fragmentation data of the respective mines. The result of the analysis showed that the interaction of the geometrical and operational parameters has increased while the interaction of the geomechanical parameters, due to being less susceptible to change of the other parameters, has decreased in the hybrid approach compared to the RES. The geomechanical parameters showed the highest impact on the system and the lowest share of interaction in the system. The geometrical and operational parameters showed a high level of interaction, in the system, which the system had low influence on them.

**Keywords** Block caving · Rock mass fragmentation · Indirect influence · Rock engineering system (RES)

## 1 Introduction

Block caving is a conventional underground extraction method as it offers advantages such as high production, low extraction costs and high automation capability. The rock mass fragmentation is important since the method is based on caving of the rock mass and its extraction out of the mining spaces. Fragmentation in block caving refers to the capability of the rock mass fracturing and breaking into

smaller fragments after it has been undercut and allowed to collapse (Catalan et al. 2010). Laubscher (2000) and Eadie (2003) have defined the fragmentation process as involving three sequential components: in situ, primary, and secondary fragmentation.

The rock mass fragmentation depends on its natural features, environmental and geometrical parameters as well as operational parameters. The estimation of fragmentation in the caving process requires enough knowledge and information on the natural fractures of the rock mass and the fragmentation which occur along the draw column. During the caving process, the fragmentation of rock mass affects the spacing and geometry of draw points, equipment selection, dilution in the draw column, the production rate at the draw points, draw control, the necessity of secondary blasting as well as the overlap of operations (Laubscher 2000).

To assess the rock mass fragmentation in a proper way, the parameters affecting the initiation and propagation of the caving and also influencing parameters on rock mass fragmentation along the draw column must be determined. The primary challenge for the development of existing

✉ Amir Azadmehr  
Azadmehr@ualberta.ca

Seyed Mohammad Esmaeil Jalali  
Sme.jalali@gmail.com

Yashar Pourrahimian  
yashar.pourrahimian@ualberta.ca

<sup>1</sup> Faculty of Mining, Petroleum and Geophysics Engineering, Shahrood University of Technology, Hafte Tir Square, Shahrood 361995161, Iran

<sup>2</sup> Department of Civil and Environmental Engineering, University of Alberta, Edmonton, Canada

methods of fragmentation forecasting is insufficient knowledge regarding the effect of influencing parameters on the process and the inability of simultaneous consideration of rock mass geomechanical, environmental, geometrical and operational features through an effective simple method.

Rock engineering system (RES) is a powerful systematic method developed by Hudson (1992), for studying the interactions among influencing parameters to solve complicated engineering problems (Hudson 1992). In the existing methods for assessment of the rock mass fragmentation, only some of influencing factors are considered, while in the RES method, not only a full list of such parameters is included, but also the interactions among parameters are considered. The RES has been used in various fields such as slope stability (Mazzoccola and Hudson 1996; Ali and Hasan 2002; Rozos et al. 2008; Zare et al. 2011; Khalokakaie and Zare 2012) and stability of tunnels (Benardos and Kaliampakos 2004; Kim 2004; Shin et al. 2009). Rafie and his colleagues have used RES to determine and evaluate the influencing parameters on caveability (Rafie et al. 2015). The RES is also used by Mohammad Khani (2014) to determine an appropriate hydraulic radius for the cave initiation at the Northparkes Mines, considering eight effective parameters in the fracturing process.

The interaction matrix as the major tool in classic RES enables a compilation of the manner in which a particular system parameter affects all other system parameters as well as the manner in which all system parameters affect that particular parameter (Hudson 2013). This basic interaction matrix, where the coupling is initially the direct binary influence between all pairs of variables, is termed the binary interaction matrix (BIM). In this BIM, we assume that  $x$  does not influence itself. This is because the BIM represents uncoupled relations. Later on, we will see that  $x$  can affect itself via a variable and mechanism pathway loop (e.g.,  $x$  affects  $y$  which in turn affects  $x$ , or there can be a loop just around the  $x$  variable itself) but this results from a subsequent coupling of the influences and does not occur in the BIM which contains only uncoupled relations between pairs of variables. We know that natural and engineered rock mechanics processes will involve more than just the isolated binary influences of subjects or parameters or variables A upon B. There will be suites of mechanisms where A affects B which affects C which affects D .... Or perhaps A affects C which affects B which affects D which then affects A, i.e., a loop from A back to A (Jiao and Hudson 1995). There will be concatenations of mechanisms, i.e., mechanism pathways, operating and we need to take them all into account, which later on is termed as indirect interaction in this study.

The indirect interaction or cross-impact of the parameters is not included in most of RES application. Matrices impact cross multiplication applied to classification method (MICMAC) is one well-known variant of cross impact

analysis (CIA) method developed by Michel godet in 1971. MICMAC analyses the importance of a given set of variables through a matrix that contains the influence that each variable has on the others (Godet 2000). Once all the influences between all the variables have been taken into account, the MICMAC provides a matrix of coefficients indicating the coupled influence of each  $x_i$  on each  $x_j$ . For example, consider that two of the variables in such a system are the normal stress,  $\sigma_n$ , across a discontinuity and the normal displacement,  $d_n$ , across the discontinuity. We can obtain a core sample through the discontinuity for a laboratory test to determine the direct binary influence of  $\sigma_n$  on  $d_n$ . However, this direct relation does not take into account how in the field, when all the relevant variables are operating, that the stress could affect the displacement indirectly through, for example, the stress affecting the water pressure which affects water flow which affects the discontinuity surface which affects the displacement.

The aim of this paper is to present a hybrid approach, which combines the classic RES and MICMAC, to examine the direct and indirect effects of influencing parameters on the rock mass fragmentation and its assessment. To this end, after introducing common methods of fragmentation prediction, the parameters affecting rock mass fragmentation are determined, the RES system is applied to the data, the ranking of the parameters is performed in both direct (RES) and indirect (MICMAC) forms. Thereafter, the indirect fragmentation index is calculated in three case studies using the hybrid approach and classification of the fragmentation index is proposed.

## 2 Literature Review

Planning for an objective production in block cave mining method is specifically affected by the reliability of draw points, which in turn are affected by appropriate fragmentation of rock mass. Various strategies have been proposed for the assessment of in situ fragmentation and several methods presented for the fragmentation estimation along the draw column (secondary fragmentation). Hustrulid and Bullock (2001) express that the fragmentation of materials must be related to the third bond theory of fragmentation, where the gravity provides the required energy for the fragmentation of the rock mass as in the downward movement of blocks in draw column, blocks with larger dimension ratios turn into smaller blocks of more stable dimension ratios. The estimation methods for distribution of fragmentation size in block caving have been based on the joint set specifications obtained via the structural mapping of outcrops or available excavations (Sainsbury and Pierce 2011).

The estimation of primary and secondary fragmentation has been usually conducted through the methods which are

based on engineering judgment and personal experiences (Esterhuizen 2005). In this regard, the utilization of Discrete Fracture Network (DFN) methods can be effective in the estimation of fragmentation including in situ, primary and secondary fragmentation. Hybrid methods using DFN have been proposed to estimate the fragmentation, but none of such methods can fully model the heterogeneity of a rock mass (Catalan et al. 2010).

Total discontinuity surfaces per unit of rock volume shows volumetric fracture intensity ( $P_{32}$ ). Rogers et al. (2014) studied the extent of the rock mass fragmentation dependance to the volumetric fracture intensity ( $P_{32}$ ) and showed the importance of the critical amount of volumetric fracture intensity ( $P_{32}$ ) where a fixed rock mass turns into a movable one.  $P_{32}$  in a DFN model depends upon a series of geomechanical features such as the average size of the block and its stiffness. Therefore, upon obtaining the  $P_{32}$  amount, some geomechanical features of rock such as fragmentation will be predictable according to the systematic relation of  $P_{32}$  with such geomechanical features (Rogers et al. 2014).

Due to the importance of fragmentation, various discontinuity models and software packages have been developed for the prediction of the size distribution of rock blocks. In some software packages such as Simblocks (Maerz and Germain 1992) and Block Cave Fragmentation (Esterhuizen 2005), the size of a joint set is assumed to be infinite. Block Cave Fragmentation (BCF) is a program, to estimate the sizes of rock fragments in draw points. The program uses a simplified technique for determining in situ block sizes and empirical rules to predict how the blocks would reduce in size in a draw column. The program was improved during 1998 and 1999 as part of the international Caving Study Stage I (Esterhuizen 2005).

The assumption of a persistence coefficient for a hypothetical joint set increases the complexity of models. The assumed continuous joint sets are divided into segments of fracture and rock bridges in a definite ratio. This model of discontinuity has been used in the estimation of in situ block size distribution (IBSD) (Latham and Lu 1999) and Makeblock (Wang et al. 2003). From among more comprehensive and complex models of DFN which include the estimation of joint set size distribution through stereological procedures, the software packages of Joints (Villaescusa and Brown 1992), Stereoblock (Hadjigeorgiou et al. 1995), Fracman (Dershowitz et al. 1998) and DFN-FRAC<sup>3D</sup> (Noroozi et al. 2015) can be mentioned.

Jing (2000) developed the basic components of an algorithm for establishing geometry of block systems of fractured rocks for discrete element methods. The algorithm is based on the basic principles of combinatorial topology and uses a boundary chain operator for block tracing, and the Euler-Poincare formula of polyhedra for ensuring the correctness of the tracing operations which has the potential and

capability to deal with any complex geometry of fracture system found in natural fractured rocks.

Lu (2002) offered an algorithm and its simulation results for the identification of rock blocks. A dynamic link list associated with the algorithm is employed to realize the representation of a polyhedron as well as its forming process by topological identification. The rock block generator is served as a pre-processor for discrete element method (DEM) using polyhedral elements or for other methods such as block theory (BT) and discontinuous deformation analysis (DDA).

Eadie (2003) offered the software of JK-FRAG for the determination of IBSD and prediction of primary fragmentation in block caving based on Harries's hierarchical joint set model. The principal assumption of this software is that in situ blocks are determined through a network of existing discontinuities in a rock mass. The software above verifies the correlation of discontinuities of a network and makes use of the mosaic method to determine primary blocks and primary fragmentation.

Call & Nicholas Company (CNI), considering the direction of drill holes in regard to the direction of major joint sets, developed Core2Frag to predict the form and volume of blocks and turn the drilling core data to the data of particle size distribution. The primary assumption for the development of primary fragmentation size distribution in drilling cores is that each part of the drilling core implies an in situ block. The relationship between the spacing of joints and the persistence of joints is studied through the features of the joint sets obtained from available excavations or targeted drilling plans, which are useful for the estimation of rock block forms (Srikant et al. 2004).

Elmoutie and Poropat (2012) outlined a method for prediction of IBSD in fractured rock masses using realistic DFN, robust polyhedral modeling, and a Monte Carlo sampling approach. The method can deal with arbitrary numbers of discontinuity sets, finite persistence representations of fractures, the consequent formation of concave polyhedral, and fracture properties described via arbitrary statistical distributions. The comparison of results of elmoutie approach with results of other approaches shows that significant differences in rock mass fragmentation estimates are possible, particularly when modeling rock masses containing discontinuity sets with low persistence.

Vyazmensky et al. (2007) made use of a hybrid code of finite-discrete element named ELFEN to apply physical fractures that gradually turned into discrete blocks to the mesh of continuous finite element (Vyazmensky et al. 2007). Due to the complexity of the model configuration and high amount of calculations for the problems in mining scale, the aforementioned hybrid method is still used in a two-dimension form. Study of related researches shows that existing methods take only a part of influencing parameters in fragmentation into consideration. On the other hand, none

of such methods consider the interactions among the influencing parameters in fragmentation. In the present research, the impact of influencing parameters and the interaction of parameters with each other and the system has been studied using RES approach, in both direct and indirect forms, and the results have been analyzed and compared to the findings of case studies.

### 3 Methodology

To design a rock engineering project for civil or mining purposes, it is very important to consider all influencing parameters and their interactions in a system. The RES is widely applied for this purpose. The major tool in RES is the interaction matrix (IM) of influencing parameters (Hudson and Harrison 2000). In the interaction matrix (Fig. 1) all major influencing parameters are arranged along the leading diagonal of the matrix, called the diagonal terms and the influence of each parameter on the other parameters is accounted for the corresponding off-diagonal positions, which are named the off-diagonal terms. To specify impacts and quantify them, the off-diagonal terms are assigned values which describe the degree of the influence of one parameter on the other parameter. Assigning these values is called coding the matrix. Different methods exist for the coding of the interaction matrix including binary, expert semi-quantitative (ESQ), Based on the slope of scatter-plot of two parameters ( $P_i$  vs.  $P_j$ ), Numerical Solution and Explicit method. ESQ has more general usage, which includes five levels of coding from zero to four (as shown in Table 1) (Hudson 2013).

The row passing through  $P_i$  represents the influence of  $P_i$  on all the other parameters in the system, while the column passing through  $P_i$  represents the influence of the rest of the system, on the  $P_i$ . After coding the interaction matrix by inserting the appropriate values for each off-diagonal cell of the matrix, For each parameter, the sum of its row values

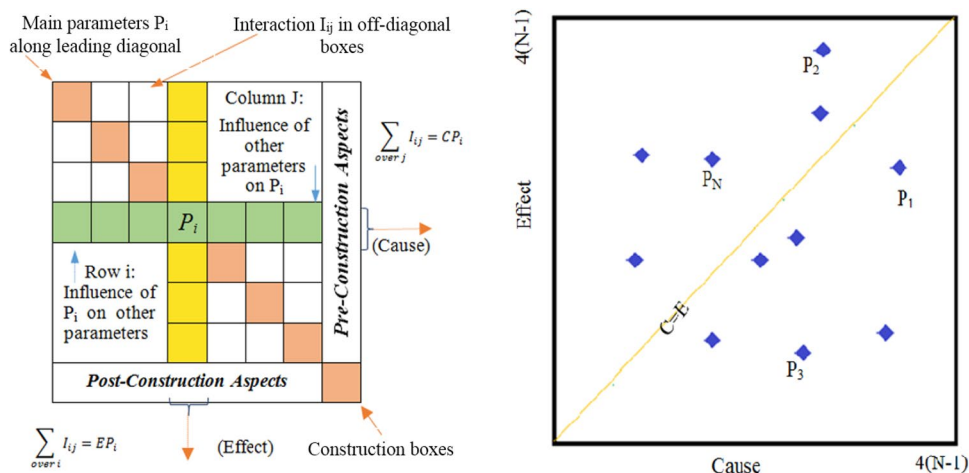
**Table 1** Meaning of points in expert semi-quantitative method

Points (code)	Meaning
Zero	Without interaction
1	Weak interaction
2	Average interaction
3	High interaction
4	Very high interaction

is termed as “Cause” ( $C_i$ ) value and the sum of its column values termed as “Effect” ( $E_i$ ) value, can be calculated which are designated as coordinates ( $C_i, E_i$ ) for a particular parameter. After obtaining the  $C \pm E$  plot for a system, it can be used for discrimination between “less interactive” and “more interactive” parameters. The position of each point in the  $C \pm E$  plot space reveals the interaction status of the respective parameter. It is obvious that the high numerical value of  $(C + E)$  shows more interaction intensity of parameter with the whole system, and the high numerical value of  $(C - E)$  shows less dominancy extent of the parameter over the system. The negative value for  $(C - E)$  reveals the dominance of the system over the respective parameter (Faramarzi et al. 2014).

Various methods have been developed to specify the indirect interaction of parameters on each other. MIC-MAC was introduced in 1992 by Godet (2000), and many of its applications have been reported. Jiao and Hudson (1995) developed a fully coupled model (FCM) based on rock engineering systems (RES) concepts and graph theory. The FCM considers the interaction matrix as a mechanism network. Graph theory is used to assess the contributions of all the mechanisms in all the pathways, a key feature being the identification of mechanism feedback loops and their stability (Jiao and Hudson 1995). Figure 2 shows various paths for the examination of the impacts of geomechanical parameters. The Page Rank

**Fig. 1** The cause–effect ( $C, E$ ) plot for the supposed case comprising  $N$  influencing parameters (Hudson 2013)



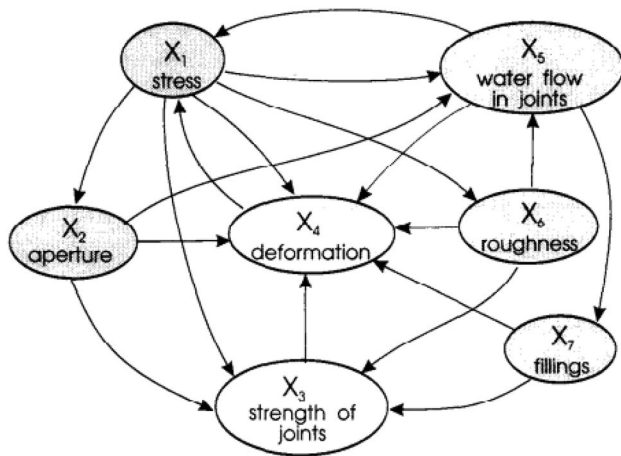


Fig. 2 Paths for examination of impacts of geomechanical parameters on each other (Jiao and Hudson 1995)

method was also presented in 1998 for computing indirect dependencies of system parameters. Chung devised Heat Kernel Method in 2007 and a sublinear time algorithm for approximating the heat kernel is presented in 2017 (Chung and Simpson 2018).

The MICMAC method has demonstrated its capabilities in diverse applications. In this method, let  $D$  be a square matrix associated with the direct influences of parameters. The indirect influences are represented by matrix  $T$  as follows:

$$T = D^k, \tag{1}$$

where  $k$  is a fixed small natural number. The vector of indirect cause  $c = (c_1, \dots, c_n)$  and the vector of indirect effect  $e = (e_1, \dots, e_n)$ , are such that their coefficients  $c_j$  and  $e_j$  are given, respectively, by:

$$c_j = \sum_{i=1}^n T_{ji}, \tag{2}$$

$$e_j = \sum_{i=1}^n T_{ij}. \tag{3}$$

Thus  $(c_j, e_j)$  is equal to the (in, out)-degree of the parameter  $j$  in the graph of indirect influences. The numbers  $c_j$  and  $e_j$  encode valuable information, for example, the most influencing variable is the one for which  $c_j$  reaches its highest value (Diaz 2013). In this study to address the indirect interaction of parameters on each other parameters, RES and MICMAC approaches have been combined and an indirect fragmentation index has been presented.

### 4 Assessment of Rock Mass Fragmentation

In this study for assessment of rock mass fragmentation, influencing parameters have been grouped into geomechanical, environmental, geometrical and operational. Geomechanical parameters include the geomechanical features of intact rock and discontinuities. The geomechanical parameters of rock mass include uniaxial compressive strength, elastic modulus, fracture frequency, discontinuity aperture, discontinuity persistence, discontinuity orientation, roughness, filling and alteration of discontinuity surfaces. Although rock mass fragmentation relies, to a large extent, on geomechanical and natural features of the rock mass, it is also significantly affected by environmental parameters such as underground water, stress field, and fine ratio. Geometrical parameters such as undercut geometry (Hydraulic Radius), undercut height, draw column height and draw points geometry, can have an influence on inductive parameters such as stress on the cave back which are effective on the rock mass fragmentation. Operational parameters are undercut direction regarding the stress direction, the draw rate and the control of draw rate at the adjacent draw points.

In total 23 influencing parameters on rock mass fragmentation have been identified and considered in this study based on literature review and discussion with experts. Thereafter, a questionnaire was prepared to establish the interaction matrix of influencing parameters on the rock mass fragmentation. The questionnaire was answered by eight experts with detailed knowledge and experience about block caving including two experts from Canada, two from Chile, one from Australia and three from Iran. The direct interaction matrix is extracted from the responded questionnaire which is shown in Table 2. Thereafter, an indirect interaction matrix ( $T$ ) is calculated using Eq. 1, while  $K$ , continuously increases from two until the system reaches a balance. The balance condition occurs when the ranking of parameters according to their influence intensity, effect intensity and interaction intensity, for two sequential series of calculations get steady. In this study after seven iterations ( $K=7$ ), the system reached a balance. It is assumed that the total interaction in the system in both RES and a hybrid approach is equal and just the weight of each parameter in the system is different among these approaches. The total interaction in RES and hybrid approach is 1545 and 600.2 e9, which is 3.9 e8 times higher in a hybrid approach. For a better comparison between two approaches, all numbers of calculated indirect interaction matrix ( $T$ ) are divided by 3.9 e8 (see Table 3). Finally, the influence, effect and interaction intensity of all influencing parameters on the rock mass fragmentation base on both methods have been calculated and presented in Table 4.

**Table 2** Interaction matrix of influential parameters in fragmentation

																				Cause	Group					
$P_1$	2	2	2	2	0	1	1	1	2	1	2	1	2	3	2	1	4	2	1	2	2	2	3	41	Geomechanical parameters	
3	$P_2$	1	2	1	0	1	1	1	2	1	3	1	1	3	3	2	3	2	1	2	2	2	3	41		
2	2	$P_3$	1	2	1	1	1	2	2	2	1	3	4	4	3	3	3	2	3	2	3	2	4	53		
1	1	1	$P_4$	1	1	2	3	2	1	1	1	3	3	2	2	1	1	1	1	1	1	2	3	37		
2	1	2	1	$P_5$	0	1	1	1	2	2	1	2	2	2	1	2	1	1	1	1	2	2	3	35		
0	0	1	1	1	$P_6$	0	1	1	2	2	1	1	0	3	3	2	1	1	0	2	3	4	3	33		
1	1	1	1	1	0	$P_7$	2	1	1	1	1	1	2	1	1	1	1	1	1	1	1	1	2	25		
1	2	0	2	1	0	2	$P_8$	2	1	1	1	1	2	1	1	1	1	0	1	1	1	1	2	26		
2	2	1	2	1	0	2	2	$P_9$	1	1	1	1	3	1	1	1	1	1	1	1	1	1	2	30		
2	1	2	1	1	3	0	1	0	$P_{10}$	1	4	2	2	4	3	3	3	3	3	3	3	3	3	50	Environmental parameters	
1	1	1	1	1	3	1	1	1	1	$P_{11}$	1	1	1	3	2	2	2	2	3	3	3	1	3	42		
0	0	1	2	1	2	1	1	1	0	0	$P_{12}$	1	0	3	3	1	2	2	1	3	0	4	3	32		
2	2	1	1	1	0	1	1	2	2	0	1	$P_{13}$	2	2	1	2	2	2	1	1	2	1	1	31		
1	1	0	0	0	0	0	0	1	1	0	0	1	$P_{14}$	1	1	2	2	4	3	1	2	3	2	26		
0	0	1	0	0	0	0	0	0	1	1	1	1	1	$P_{15}$	2	3	2	2	1	3	3	1	3	26	Geometrical parameters	
0	0	1	0	0	0	0	0	0	2	1	1	1	2	3	$P_{16}$	2	1	2	1	3	2	1	3	26		
0	0	0	0	0	0	0	0	0	1	1	1	1	3	3	1	$P_{17}$	4	4	3	3	3	2	3	33		
0	0	0	0	0	0	0	0	0	1	1	0	1	2	1	0	3	$P_{18}$	4	3	1	4	1	2	24		
0	0	1	1	0	0	0	0	0	2	1	1	1	3	0	0	3	2	$P_{19}$	4	4	3	2	3	31	Operational parameters	
0	0	0	0	0	0	0	0	0	2	1	1	1	2	0	0	2	1	2	$P_{20}$	3	2	2	2	21		
0	0	1	0	0	0	0	0	0	2	1	0	1	1	0	0	1	2	1	2	$P_{21}$	2	1	3	18		
0	0	0	0	0	0	0	0	0	1	0	0	1	1	0	0	1	0	2	2	2	$P_{22}$	1	2	13		
0	1	0	0	0	0	0	0	0	2	2	2	1	1	0	1	1	2	2	2	1	1	$P_{23}$	2	21		
0	0	0	0	0	0	0	0	0	0	0	0	0	0	2	1	1	2	0	3	1	2	3	0	$P_{24}$	15	system
18 17 18 18 14 10 13 16 16 32 22 25 28 42 41 32 42 41 46 40 47 50 39 60																				Effect						

$P_1/UCS$  uniaxial compressive strength,  $P_2/E_m$  elastic modulus,  $P_3/FF$  fracture frequency,  $P_4/D_{Ap}$  discontinuity aperture,  $P_5/D_{Per}$  discontinuity persistence,  $P_6/D_{Dir}$  discontinuity direction,  $P_7/D_{Rou}$  discontinuity roughness,  $P_8/D_{Fi}$  discontinuity filling,  $P_9/D_{Alt}$  discontinuity alteration,  $P_{10}/S_{Field}$  stress field,  $P_{11}/SD$  stress direction,  $P_{12}/S_{Ra}$  stress ratio,  $P_{13}/GW$  ground water,  $P_{14}/FMR$  fine material ratio,  $P_{15}/HR$  hydraulic radius,  $P_{16}/UH$  undercut height,  $P_{17}/DCH$  draw column height,  $P_{18}/DPG$  draw point geometry,  $P_{19}/D_{Ra}$  draw rate,  $P_{20}/MDI$  multiple draw interaction,  $P_{21}/AG$  air gap,  $P_{22}/BOD$  broken ore density,  $P_{23}/UD$  undercutting direction,  $P_{24}/Fg$  fragmentation

The following points are concluded based on the results of interaction matrices:

- According to the Table 3 in a hybrid approach, the value of diagonal terms is not zero which means that each parameter has also effect on itself, for example, the influence of parameter  $P_1$  on itself is 0.71 which is a weak interaction.
- The interaction of some parameters with others has significantly changed in a hybrid approach. For example, the effect of  $P_3$  on  $P_{19}$  is changed from two to 4.4. In other words, the effect of  $P_3$  on  $P_{19}$  is changed from category 4 (very high interaction) to category two (average interaction).
- According to Table 4, the maximum increase (11.6%) and maximum decrease (15.5%) in case of influencing parameters in the hybrid approach are related to underground water and draw column height, respectively.
- The maximum increase (28.9%) and maximum decrease (49.2%) in effect of influencing parameters in the hybrid approach belong to draw rate and joint roughness, respectively.
- The maximum increase in indirect interaction intensity of influencing parameter mainly belongs to operational parameters including multiple draw interaction and draw rate with 18.9% and 13.8% change, respectively.

**Table 3** Indirect interaction matrix of influential factors (using MICMAC approach)

	$P_1$	$P_2$	$P_3$	$P_4$	$P_5$	$P_6$	$P_7$	$P_8$	$P_9$	$P_{10}$	$P_{11}$	$P_{12}$	$P_{13}$	$P_{14}$	$P_{15}$	$P_{16}$	$P_{17}$	$P_{18}$	$P_{19}$	$P_{20}$	$P_{21}$	$P_{22}$	$P_{23}$	$P_{24}$	C
$P_1$	0.71	0.7	0.9	0.69	0.48	0.53	0.4	0.51	0.58	2.06	1.25	1.37	1.63	2.76	2.06	1.55	2.94	2.62	3.55	3.16	3.36	3.56	2.38	3.76	43.51
$P_2$	0.7	0.69	0.89	0.69	0.48	0.53	0.39	0.51	0.58	2.04	1.24	1.36	1.62	2.73	2.04	1.54	2.91	2.59	3.52	3.14	3.34	3.53	2.36	3.73	43.15
$P_3$	0.88	0.86	1.12	0.86	0.6	0.66	0.49	0.63	0.72	2.55	1.55	1.7	2.03	3.42	2.55	1.92	3.64	3.24	4.4	3.92	4.17	4.42	2.95	4.66	53.94
$P_4$	0.63	0.62	0.8	0.61	0.43	0.47	0.35	0.45	0.52	1.82	1.1	1.21	1.44	2.43	1.82	1.37	2.59	2.31	3.13	2.79	2.97	3.14	2.1	3.32	38.42
$P_5$	0.62	0.61	0.79	0.61	0.42	0.47	0.35	0.45	0.51	1.81	1.1	1.21	1.44	2.43	1.81	1.36	2.58	2.3	3.12	2.78	2.96	3.13	2.09	3.31	38.26
$P_6$	0.53	0.52	0.68	0.52	0.36	0.4	0.3	0.38	0.44	1.55	0.94	1.03	1.23	2.08	1.55	1.17	2.21	1.97	2.68	2.38	2.53	2.68	1.79	2.83	32.75
$P_7$	0.44	0.44	0.56	0.43	0.3	0.33	0.25	0.32	0.37	1.29	0.78	0.86	1.02	1.73	1.29	0.97	1.84	1.64	2.22	1.98	2.11	2.23	1.49	2.36	27.25
$P_8$	0.46	0.46	0.59	0.45	0.32	0.35	0.26	0.33	0.38	1.34	0.81	0.89	1.07	1.8	1.34	1.01	1.92	1.71	2.32	2.06	2.19	2.32	1.55	2.45	28.38
$P_9$	0.55	0.54	0.7	0.53	0.37	0.41	0.31	0.39	0.45	1.59	0.96	1.06	1.26	2.13	1.59	1.2	2.27	2.02	2.74	2.44	2.6	2.75	1.84	2.9	33.6
$P_{10}$	0.82	0.8	1.04	0.8	0.56	0.61	0.46	0.59	0.67	2.38	1.44	1.58	1.89	3.18	2.38	1.79	3.39	3.02	4.1	3.65	3.88	4.11	2.75	4.35	50.24
$P_{11}$	0.62	0.61	0.79	0.61	0.42	0.47	0.35	0.45	0.51	1.81	1.1	1.2	1.44	2.42	1.81	1.36	2.58	2.3	3.12	2.78	2.95	3.13	2.09	3.3	38.22
$P_{12}$	0.5	0.49	0.64	0.49	0.34	0.38	0.28	0.36	0.41	1.46	0.88	0.97	1.16	1.95	1.46	1.1	2.08	1.85	2.51	2.24	2.38	2.52	1.68	2.66	30.79
$P_{13}$	0.56	0.55	0.72	0.55	0.38	0.42	0.32	0.41	0.46	1.64	0.99	1.09	1.3	2.19	1.64	1.23	2.33	2.08	2.82	2.51	2.67	2.83	1.89	2.99	34.57
$P_{14}$	0.4	0.39	0.51	0.39	0.27	0.3	0.22	0.29	0.33	1.16	0.7	0.77	0.92	1.55	1.15	0.87	1.65	1.47	1.99	1.77	1.89	2	1.33	2.11	24.43
$P_{15}$	0.38	0.38	0.49	0.37	0.26	0.29	0.21	0.27	0.31	1.11	0.67	0.74	0.88	1.49	1.11	0.84	1.59	1.41	1.92	1.71	1.82	1.92	1.28	2.03	23.48
$P_{16}$	0.4	0.4	0.51	0.39	0.27	0.3	0.23	0.29	0.33	1.17	0.71	0.78	0.93	1.57	1.17	0.88	1.67	1.49	2.02	1.8	1.92	2.03	1.36	2.14	24.76
$P_{17}$	0.45	0.45	0.58	0.44	0.31	0.34	0.25	0.33	0.37	1.32	0.8	0.88	1.05	1.77	1.32	0.99	1.88	1.67	2.27	2.02	2.15	2.28	1.52	2.41	27.85
$P_{18}$	0.34	0.34	0.43	0.33	0.23	0.26	0.19	0.25	0.28	0.99	0.6	0.66	0.79	1.33	0.99	0.75	1.42	1.26	1.71	1.52	1.62	1.72	1.15	1.81	20.97
$P_{19}$	0.46	0.45	0.59	0.45	0.31	0.35	0.26	0.33	0.38	1.34	0.81	0.89	1.06	1.8	1.34	1.01	1.91	1.7	2.31	2.06	2.19	2.32	1.55	2.45	28.32
$P_{20}$	0.32	0.32	0.41	0.31	0.22	0.24	0.18	0.23	0.27	0.94	0.57	0.62	0.74	1.25	0.94	0.7	1.33	1.19	1.61	1.44	1.53	1.62	1.08	1.71	19.77
$P_{21}$	0.29	0.28	0.36	0.28	0.19	0.21	0.16	0.21	0.24	0.83	0.5	0.55	0.66	1.11	0.83	0.63	1.19	1.06	1.43	1.28	1.36	1.44	0.96	1.52	17.57
$P_{22}$	0.19	0.19	0.24	0.19	0.13	0.14	0.11	0.14	0.16	0.56	0.34	0.37	0.44	0.74	0.55	0.42	0.79	0.71	0.96	0.85	0.91	0.96	0.64	1.01	11.74
$P_{23}$	0.36	0.35	0.45	0.35	0.24	0.27	0.2	0.26	0.29	1.03	0.63	0.69	0.82	1.38	1.03	0.78	1.47	1.31	1.78	1.59	1.69	1.79	1.19	1.89	21.84
$P_{24}$	0.2	0.2	0.25	0.19	0.14	0.15	0.11	0.14	0.16	0.58	0.35	0.38	0.46	0.77	0.58	0.43	0.83	0.74	1	0.89	0.95	1	0.67	1.06	12.23
E	11.81	11.64	15.04	11.53	8.03	8.88	6.63	8.52	9.72	34.37	20.82	22.86	27.28	46.01	34.35	25.87	49.01	43.66	59.23	52.76	56.14	59.43	39.69	62.76	

$P_1/UCS$  uniaxial compressive strength,  $P_2/E_m$  elastic modulus,  $P_3/FF$  fracture frequency,  $P_4/D_{Ap}$  discontinuity aperture,  $P_5/D_{Per}$  discontinuity persistence,  $P_6/D_{Dir}$  discontinuity direction,  $P_7/D_{Rou}$  discontinuity roughness,  $P_8/D_{Fi}$  discontinuity filling,  $P_9/D_{Alt}$  discontinuity alteration,  $P_{10}/S_{Field}$  stress field,  $P_{11}/SD$  stress direction,  $P_{12}/S_{Ra}$  stress ratio,  $P_{13}/GW$  ground water,  $P_{14}/FMR$  fine material ratio,  $P_{15}/HR$  hydraulic radius,  $P_{16}/UH$  undercut height,  $P_{17}/DCH$  draw column height,  $P_{18}/DPG$  draw point geometry,  $P_{19}/D_{Ra}$  draw rate,  $P_{20}/MDI$  multiple draw interaction,  $P_{21}/AG$  air gap,  $P_{22}/BOD$  broken ore density,  $P_{23}/UD$  undercutting direction,  $P_{24}/Fg$  fragmentation, C cause, E effect

As shown in Table 4, the influence intensity of most geomechanical parameters increases in the hybrid method. Moreover, the quantity of effect intensity of geomechanical and environmental parameters has significantly dropped, which is in accord with the low susceptibility of geomechanical parameters to operational parameters and human interference. On the other hand, the quantity of the effect and interaction intensity of both geometrical and operational parameters have clearly risen in the hybrid method. While studying the interaction of the parameters in Table 4, it is noticed that the geometrical and operational parameters have significantly changed in the hybrid method compared to the direct method. Since the geometrical and operational parameters can be modified and revised in all stages of mining design, fragmentation of rock mass could be improved by applying changes to the parameters of these two groups. Figure 3 shows the histogram of influence intensity, effect intensity and the indirect interaction intensity of the influencing parameters on the rock mass fragmentation. The results show that the frequency of discontinuities, the in situ stresses, uniaxial compressive strength, and Young’ modulus are, respectively, the most influencing parameters of the system. Furthermore, broken ore density, the height of the

air gap, and the Multiple Draw interaction have, respectively, lowest influence on the system.

Figure 4 shows that the indirect impact of geomechanical parameters is higher than their direct impact. In the environmental parameters group, the indirect influence of parameters is somewhat lower than the influence of the direct method, except for the influence of underground water, which shows an approximate increase of 5%.

In most geometrical and operational parameters, the indirect influence of parameters is lower than their direct impact except for the parameter of air gap height and undercutting direction whose weight in the system is somewhat higher than direct influence.

In Fig. 5, a comparison of the system dominancy over parameters in two direct and indirect forms could be seen. In the group of geomechanical parameters, the indirect dependency of parameters is considerably lower than the direct one. Moreover, in the environmental group, the indirect dependency of the in situ stresses field is lower than its direct type, and for the other parameters of the group, it is negligible. The indirect dependency amount of geometrical and operational parameters for most parameters is higher than their direct dependency.

**Table 4** Cause, effect, and interaction ( $C+E$ ) of influencing parameters in fragmentation and percent of changes in the direct and indirect method

Group	Parameters	Cause			Effect			Cause+Effect		
		Direct	Indirect	Change (%)	Direct	Indirect	Change (%)	Direct	Indirect	Change (%)
Geomechanical	Uniaxial Compressive strength	41	43.5	6.1	18	11.8	-34.4	59	55.4	-6.1
	Modulus ratio	41	43.2	5.4	17	11.6	-31.8	58	54.8	-5.5
	Fracture Frequency	53	53.9	1.7	18	15	-16.7	71	69	-2.8
	Discontinuity Aperture	37	38.4	3.8	18	11.5	-36.1	55	49.9	-9.3
	Discontinuity Persistence	35	38.3	9.4	14	8.1	-42.1	49	46.3	-5.5
	Discontinuity Orientation	33	32.8	-0.6	10	8.9	-11	43	41.6	-3.3
	Joint Roughness (JRC)	25	27.3	9.2	13	6.6	-49.2	38	33.9	-10.8
	Filling	26	28.4	9.2	16	8.5	-46.9	42	36.9	-12.1
	Joint surface alteration	30	33.6	12	16	9.7	-39.4	46	43.4	-5.7
Environmental	In-situ stresses	50	50.3	0.6	32	34.4	7.5	82	84.6	3.2
	Stresses Orientation	42	38.2	-9	22	20.8	-5.5	61	59	-3.3
	Stress Ratio	32	30.8	-3.8	25	22.9	-8.4	57	53.7	-5.8
	Underground water	31	34.6	11.6	28	27.3	-2.5	59	61.9	4.9
	Fine Materials Ratio	26	24.4	-6.2	42	46	9.5	68	70.4	3.5
Geometrical	Hydraulic Radius	26	23.5	-9.6	41	34.3	-16.3	67	57.8	-13.7
	Undercut Height	26	24.8	-4.6	32	25.8	-19.4	58	50.6	-12.8
	Draw Column Height	33	27.9	-15.5	42	49	16.7	75	76.9	2.5
	Draw Points Geometry	24	21	-12.5	41	43.7	6.6	65	64.6	-0.6
Geometrical	Draw Rate	31	28.3	-8.7	46	59.3	28.9	77	87.6	13.8
	Multiple Draw Interaction	21	19.8	-5.7	40	52.8	32	61	72.5	18.9
	Air gap Height	18	17.6	-2.2	47	56.1	19.4	65	73.7	13.4
	ility	13	11.7	-10	50	59.4	18.8	63	71.2	13
	Undercut Direction	21	21.8	3.8	39	39.7	1.8	60	61.5	2.5
System	Fragmentation	15	12.2	-18.7	60	62.8	4.7	75	75	0

Figure 6 refers to a comparison of the indirect-to-direct interactions of the influencing parameters of the system. The indirect interaction of geomechanical parameters is somewhat lower than their direct interaction. Besides, in the environmental group, the indirect interaction of parameters makes little difference from the direct one. Only the indirect interaction of the parameters of the stress field and underground water scarcely exceeds the direct interaction. Since from among environmental parameters, only the above two parameters are controllable, if necessary, there could be created a significant change in the rock mass fragmentation

through some contrivance such as hydraulic fracturing, vertical cuts at the block borders, dewatering, etc.

In the group of geometrical and operational parameters, for most parameters, a significant increase can be seen in the indirect interaction compared to the direct one. Only two parameters including undercut height and hydraulic radius reveal a 10% drop in the indirect interaction. Therefore, by making changes to geometrical and operational parameters, especially to the draw rate, and its control through the neighboring draw points which have the highest interaction with the system, the fragmentation extent could be controlled.



**Fig. 3** Histogram of cause, effect and interaction intensity in Hybrid method

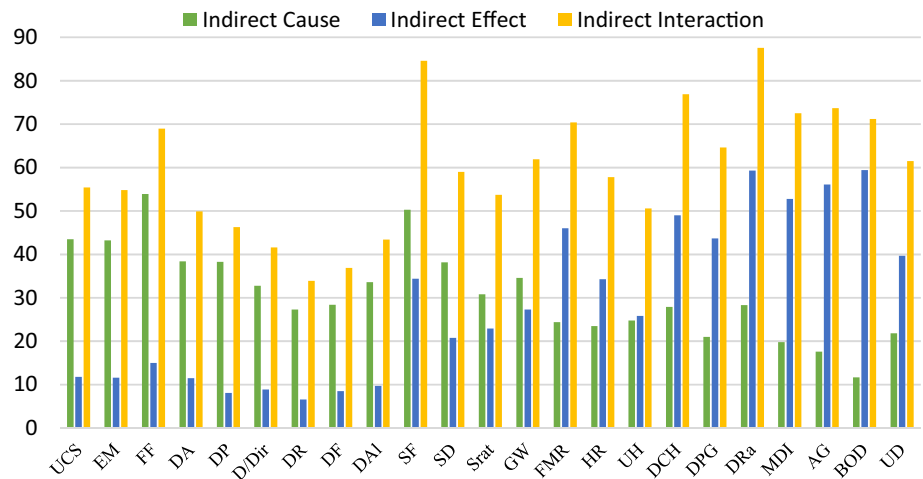


**Fig. 4** Comparison of direct and indirect influence intensity of influencing parameters on block caving

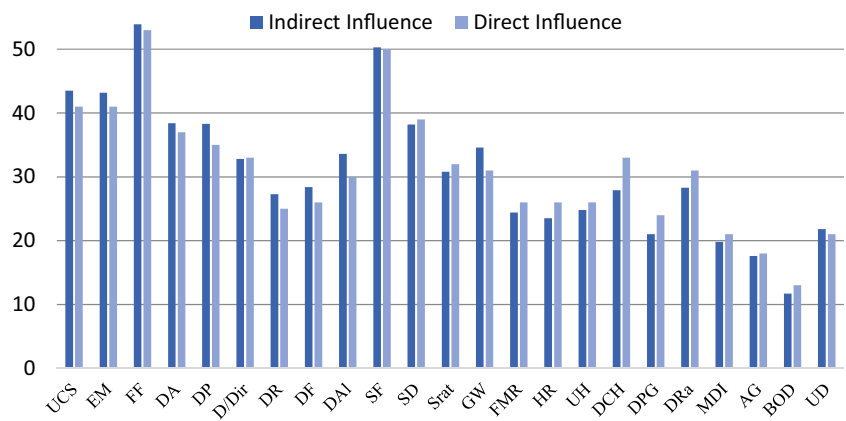


**Fig. 5** Comparison of direct and indirect effect intensity of influencing parameters on block caving

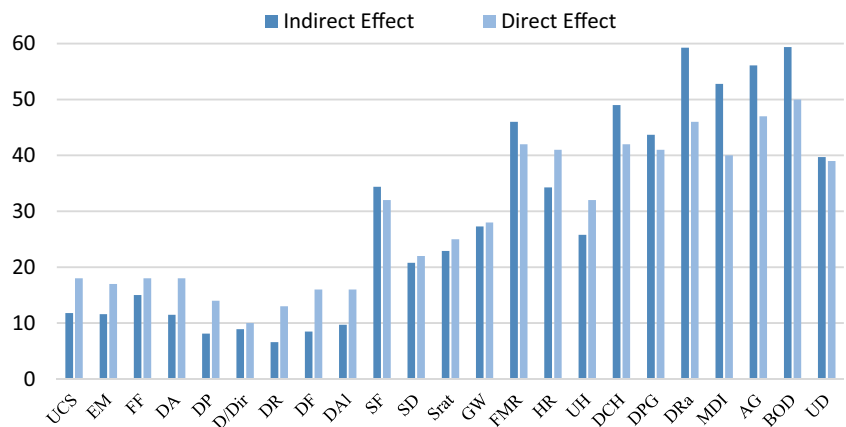
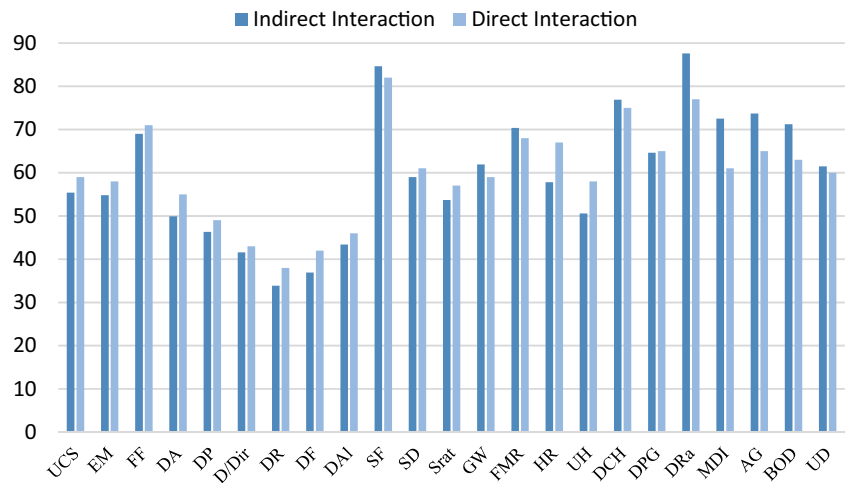


Table 5 shows the ranking of the influencing parameters on the rock mass fragmentation based on influence, effect, and interaction for both direct and hybrid methods. A study of Figs. 3, 4, 5, and 6, as well as Table 5, shows that the ranking of parameters, i.e., the parameters' weight, is different at direct and indirect methods. For example, in terms of the parameters' interaction, the fracture frequency, having dropped as many as 4 levels, lies in the

ninth position of indirect interaction while the Multiple Draw Interaction has reached the 6th place after rising of 6 stages from the 12th place.

To determine a fragmentation index, there is a necessity for ranking and assigning proper codes for the influencing parameters on fragmentation for each of case studies. Table 6 is developed for classification and coding

**Fig. 6** Comparison of direct and indirect interaction intensity of influencing parameters on block caving



**Table 5** Comparison of ranking of influencing parameters in fragmentation in direct and indirect methods

Interaction ranking			Influence ranking			Effect ranking		
Direct	order	Indirect	Direct	order	Indirect	Direct	order	Indirect
SF	1	D <sub>Ra</sub>	FF	1	FF	Frg	1	Frg
D <sub>Ra</sub>	2	SF	SF	2	SF	BOD	2	BOD
DCH	3	DCH	S <sub>Dir</sub>	3	UCS	AG	3	D <sub>Ra</sub>
Frg	4	Frg	UCS	4	EM	D <sub>Ra</sub>	4	AG
FF	5	AG	EM	5	D <sub>iAp</sub>	FMR	5	MDI
FMR	6	MDI	D <sub>iAp</sub>	6	D <sub>iPer</sub>	DCH	6	DCH
HR	7	BOD	D <sub>iPer</sub>	7	S <sub>Dir</sub>	HR	7	FMR
DPG	8	FMR	D <sub>iDir</sub>	8	GW	DPG	8	DPG
AG	9	FF	DCH	9	D <sub>iAlt</sub>	MDI	9	U <sub>Dir</sub>
BOD	10	DPG	S <sub>Rat</sub>	10	D <sub>iDir</sub>	U <sub>Dir</sub>	10	SF
SD	11	GW	GW	11	S <sub>Rat</sub>	SF	11	HR
MDI	12	U <sub>Dir</sub>	D <sub>Ra</sub>	12	D <sub>iFill</sub>	UH	12	GW
U <sub>Dir</sub>	13	SD	D <sub>iAlt</sub>	13	D <sub>Ra</sub>	GW	13	UH
UCS	14	HR	D <sub>iFill</sub>	14	DCH	S <sub>Rat</sub>	14	S <sub>Rat</sub>
GW	15	UCS	FMR	15	D <sub>iRou</sub>	S <sub>Dir</sub>	15	S <sub>Dir</sub>
EM	16	EM	HR	16	UH	UCS	16	FF
UH	17	S <sub>Rat</sub>	UH	17	FMR	FF	17	UCS
S <sub>Rat</sub>	18	UH	D <sub>iRou</sub>	18	HR	D <sub>iAp</sub>	18	EM
D <sub>iAp</sub>	19	D <sub>iAp</sub>	DPG	19	U <sub>Dir</sub>	EM	19	D <sub>iAp</sub>
D <sub>iPer</sub>	20	D <sub>iPer</sub>	MDI	20	DPG	DF	20	D <sub>iAlt</sub>
D <sub>iAlt</sub>	21	D <sub>iAlt</sub>	U <sub>Dir</sub>	21	MDI	D <sub>iAlt</sub>	21	D <sub>iDir</sub>
D <sub>iDir</sub>	22	D <sub>iDir</sub>	AG	22	AG	D <sub>iPer</sub>	22	D <sub>iFill</sub>
D <sub>iFill</sub>	23	D <sub>iFill</sub>	Frg	23	Frg	D <sub>Ra</sub>	23	D <sub>iPer</sub>
D <sub>iRou</sub>	24	D <sub>iRou</sub>	BOD	24	BOD	D <sub>iDir</sub>	24	D <sub>iRou</sub>

of influencing parameters on rock mass fragmentation. Development of Table 6 is based on the following points:

- For parameters including UCS, Em, FF,  $D_{Ap}$ ,  $D_{Per}$ ,  $D_{Dir}$ ,  $D_{Rou}$ ,  $D_{Fi}$ ,  $D_{Alt}$ , and UD, similar approach of rock mass classification system (IRM, MRMR, and their adjustments) was used (Laubscher and Jakubec 2000; Brown 2003), for example with regard to UCS, it is divided into four categories similar to MRMR classification but for higher UCS, a lower score is assigned.

- Scoring for parameters like BOD, DCH, UH, DRa, and MDI, has been done by reviewing existing researches in these fields (Pierce 2010; Dorador et al. 2014; Gomez et al. 2017).
- For parameters including AG, FMR, DCH,  $S_{Field}$ ,  $S_{Ra}$ , and UD, sensitivity analysis has been done by the use of BCF software and using a PFC model developed by the author.
- Also, the suggestion of experts has been used for determining and refining scoring ranges.

**Table 6** Classification and coding of influencing parameters in fragmentation

Row	Parameter	Unit	Class (code)				
			0	1	2	3	4
1	Uniaxial compressive strength	MPa	> 100	70–100	40–70	25–40	< 25
2	Modulus ratio	–	< 100	100–200	200–300	300–400	> 400
3	Fracture frequency	1/m	< 1	1–3	3–5	5–8	> 8
4	Aperture	mm	Without opening	< 1	1–3	3–5	> 5
5	Persistence	m	< 0.5	0.5–1.5	1.5–3	3–5	> 5
6	Joints orientation	–	Very unfavorable	Unfavorable	Fair	Favorable	Very favorable
7	Roughness (JRC)	–	15–20	10–15	5–10	2–5	< 2
8	Filling	mm	Very hard filling	Very hard filling > 5 mm	Without filling	Soft filling < 5	Soft and very soft filling > 5
9	Weathering	–	Without weathering	Few weathering	Rather weathered	Weathered	Strongly weathered
10	In situ stresses	MPa	< 5	5–10	10–15	15–20	> 20
11	Stresses orientation	Degree	Perpendicular to joint set	63°–80° according to joint set	45°–63° according to joint set	20°–45° according to joint set	Parallel to joint set
12	Stress ratio	–	< 1	1–1.5	1.5–2	2–2.5	> 2.5
13	Underground water	–	Completely dry	Damp	Wet	Dripping	Flowing
14	Fine ratio	%	> 20	15–20	10–15	5–10	< 5
15	Hydraulic radius	m	< 15	15–30	30–45	45–60	> 60
16	Undercut height	m	< 4	4–6	6–8	8–12	> 12
17	Draw column height	m	< 50	50–100	100–150	150–200	> 200
18	Draw points geometry	$S_{up}/S_{low}$	< 2	2–3	3–4	4–6	> 6
19	Draw rate	Mm/day	> 250	200–250	150–200	100–150	< 100
20	Multiple draw interaction	–	Isolated draw	Coincidental draw of 2 adjacent draw points	Coincidental draw of 4 adjacent draw points	Coincidental draw of 6 adjacent draw points	Coincidental draw of 8 adjacent draw points
21	Air gap height	m	Negligible	< 2	2–4	4–6	> 6
22	Broken ore density	–	< 1.2	1.2–1.4	1.4–1.6	1.6–1.8	> 1.8
23	Undercut direction	–	Very unfavorable	Unfavorable	Fair	Favorable	Very favorable

The ranking of joint set orientation and undercut direction has been presented qualitatively in Table 6. Therefore, a description of the quality of joint set orientation in block caving, as well as the orientation of undercut, is, respectively, presented in Tables 7 and 8.

## 5 Fragmentation Assessment of Case Studies

Reserve North (ReNo) and Diablo Regimiento from El Teniente deposit and Kemess Mines were selected for case studies due to difference in their geological structures and rock mass features, leading to the different types of fragmentation. Here, these mines are introduced in brief.

*El Teniente Mine* El Teniente is the world's biggest underground copper deposit, located 70 km southeast from

Santiago in the Andes mountain range in Chile. The actual depth of copper mineralization at the El Teniente Mine is not known and only its propagation to a depth of over 1300 m has been proven. Due to the vast area, the existing underground mine comprises six mining blocks around the Braden Pipe at different elevations including the Esmeralda, Reservas Norte, Diablo Regimiento and Pipa Norte mining blocks (Brazovic and Villaescusa 2007). The Reservas Norte (ReNo), and Diablo Regimiento sectors were selected for fragmentation evaluation.

The Diablo Regimiento mining block is located in the south of El Teniente orebody. The maximum block height is 600 m at the northern end of this sector while the average height is approximately 150 m in this area. The average daily extraction rate is 28,000 tons per day, with an extraction rate of 0.3–0.6 ton per square meter and an annual undercut rate of 30,000 m<sup>2</sup>.

**Table 7** Evaluation of joint set orientation quality in block caving mines

Very unfavorable	Unfavorable	Fair	Favorable	Very favorable
Two of joints sets or less with the slope of 60–90 degree	Two joint sets One set is relatively perpendicular The others with the slope of 30°–60°	At least three joint sets One group with a slope of 10°–30° (the direction of the slope is against the direction of undercut) Two sets with a slope above 60°	At least three joint sets One set with the slope of 10°–30° (the direction of the slope is the same as that of the undercut) Two sets with cross each other with a slope above 60°	At least three joint sets One set with the slope of 0°–10° Two others crossing each other with a slope above 60°

**Table 8** The evaluation of the undercut condition in block caving mines

Very unfavorable	Unfavorable	Fair	Favorable	Very favorable
Undercutting against the direction of maximum main stress; from the hard rocks toward the soft ones with irregular forehead	Undercutting against the direction of maximum main stress; from the hard rocks toward the softs with regular forehead	Undercutting with no respect to the maximum main stress; from the weak rocks toward the hard ones or from the pre caving extracted blocks	Undercutting in the direction of maximum main stress; from the weak rocks toward the hard ones	Undercutting in the direction of maximum main stress; from the weak rocks toward the hard ones or toward a perpendicular cut in the margin of an ore body

The ReNo mining block is located in the north of El Teniente orebody. Its undercut is around 27,000 m<sup>2</sup> with a hydraulic radius of 36. The height of the caving column is 190 m on average (Brazovic and Villaescusa 2007).

**Kemess Mine** The Kemess Mine is a porphyry deposit containing copper, gold and silver minerals, located in a mountainous region in the central north of the British Columbia in Canada, 250 km north of the City of Smithers. The mining area lies in the depth of 200–550 m off the ground level. The optimal undercut level at the Kemess Mine has been estimated in the depth of 550 m, in approximate dimensions of 550 m east–west and 90–300 m north–south. The design of this mine is based on an annual production of 9 million tons (Jakubec et al. 2016). To estimate the fragmentation of the Kemess Mine in the phase of the feasibility study, the block caving fragmentation (BCF) software was used (Jakubec et al. 2016).

Figure 7 shows the fragmentation size distribution diagram for the Kemess Mine at the various draw column heights of 20, 50, 100, and 200 m and the draw rate of 10 cm per day. The red line represents the primary fragmentation; the blue line represents the secondary fragmentation for 20 m draw height up to the green curve, which represents the secondary fragmentation at the draw column height of 200 m. The cumulative percentage of the blocks larger than 1 and 2 m<sup>2</sup>, given the respective curve at the draw column height of 100 m (black color) was reported 21% and 14%, respectively.

The cumulative percentage of the blocks larger than one and two cubic meters in the ReNo and Diablo Regimiento mines is reported in Table 9. The results show that the Kemess Mine, with 14% of the blocks larger than two cubic meters, has the highest potential of fragmentation followed in the next ranks by the ReNo and Diablo Regimiento mines, with 27 and 33% of the blocks larger than 2 cubic meters.

According to rock mass specifications, data and information of the three mines under study and based on codes are

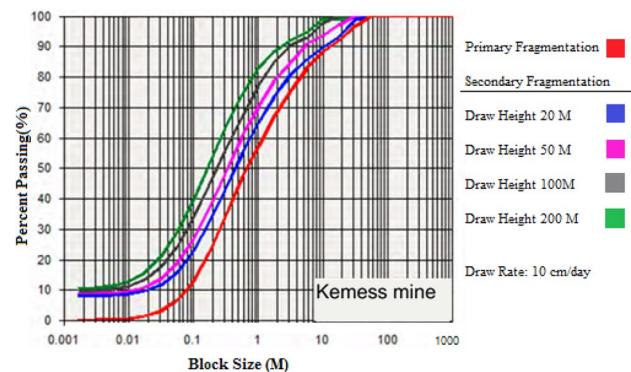


**Fig. 7** Block size distribution at draw points in Kemess Mine using BCF (Jakubec et al. 2016)

**Table 9** Percent of fragments larger than 1 m<sup>3</sup> and 2 m<sup>3</sup>

Row	Mine	Blocks volume at draw points	
		> 2 m <sup>3</sup> (%)	> 1 m <sup>3</sup> (%)
1	ReNo	27	31
2	Diablo Regimiento	33	35
3	Kemess	14	21

presented in Table 6 all the influencing parameters have been scored for each case study and the results are presented in Table 10. An average point of two was assigned for the three parameters including multiple draw interaction, the broken ore density, and the air gap height, due to the unavailability of exact data in the reports.

Then, the calculations for the determination of rock mass fragmentation index were conducted for all the three case studies (see Table 11). The amounts of fragmentation indexes for the ReNo, Diablo Regimiento, and Kemess mines were obtained as 58.76, 49.54, and 59.90%, respectively. The results show that the Kemess Mine and Diablo Regimiento mines have, respectively, the highest and the lowest fragmentation potential. Mining engineers can improve the fragmentation by considering proper design parameters, especially operational parameters. As an example, by considering the point 4, instead of average point of two (as mentioned in previous paragraph), for multiple draw interaction, the broken ore density and the air gap height (Table 10), the fragmentation index for ReNo, Diablo Regimiento and Kemess mines could be increased up to 66.66, 57.44, and 67.78 percent, respectively.

Maximum, minimum and mean share of influence, effect and interaction intensities in each group of influencing parameters have presented in Table 12. Geomechanical parameters hold the highest influence and interaction intensity in the system with the approximate share amount of 47.53 and 31.3%, respectively. The highest influence intensity belongs to the fracture frequency from the geomechanical group while the lowest influence intensity belongs to the broken ore density from the group of operational parameters. The average share of influence for the parameters of each group has been calculated and according to the results, the geomechanical parameters have the highest average influence in each group, with an amount of 5.28%.

As for the effect intensity, operational parameters, with a total approximate amount of 40.30% showed the highest weight in the system, followed in the next rank by geometric, environmental, and geomechanical parameters, each with a weight of 23.04, 22.84, and 13.82 percent, respectively. The parameter of the broken ore density and the roughness of the discontinuity surface had the highest share of 8.96% in the group of operational parameters and the lowest share of the effect of 1% from the system. The operational parameters

**Table 10** Points dedicated to influencing parameters in fragmentation base on existing data

Row	Parameter	Unit	ReNo mine		Diablo Regimiento mine		Kemess mine	
			Quantity	Point	Quantity	Point	Quantity	Point
1	Uniaxial compressive strength	MPa	120	0	116	0	106	0
2	Modulus ratio	–	450	4	> 500	4	295	2
3	Fracture frequency	/m	6.53	3	2	1	¾	2
4	Discontinuity aperture	Mm	<2	2	> 3	3	1–5	3
5	Discontinuity persistence	Meter	2.46	2	1.60	2	Semi continuous	4
6	Discontinuity orientation	–	Very favorable	4	Favorable	3	Favorable	3
7	Discontinuity roughness	–	Rough	1	Rough	1	Relatively rough	2
8	Infilling	Mm	Very hard	0	Soft > 5	3	Soft	3
9	Alteration	–	Slightly	1	Slightly	1	No	0
10	Stress field	MPa	35	4	25	4	15–20	3
11	Stress orientation	°	20–45	3	20–45	3	Low	3
12	Stress ratio	–	2–3	3	2.1	3	2–4	4
13	Underground water	–	Dry	0	Wet	1	12 l/s	4
14	Fine ratio	%	30	1	30	1	30	1
15	Hydraulic radius	M	36	2	38	2	33	2
16	Undercut height	M	4	1	4	1	18	4
17	Draw column height	M	190	3	109	2	100	1
18	Draw points geometry	$S_{up}/S_{low}$	4.86	3	4.1	3	4	3
19	Draw rate	Mm/day	70–100	4	330	0	200	2
20	Multiple draw interaction	–	Favorable	4	Favorable	4	Favorable	4
21	Air gap height	M	10	4	10	4	10	4
22	Broken ore density	–	1.4	2	1.4	2	1.4	2
23	Direction of undercut	–	In suit with	4	Medium	2	In suit with	4

have the highest share of effect on average. The geomechanical and geometrical parameters, respectively, have the highest (31.3%) and lowest (18.14%) interactions with the system.

Given that the mines under study have acceptable fragmentation potential, a comparison of the findings of the hybrid method to the data obtained from the respective mines makes it possible to offer a ranking (as shown in Table 13), for fragmentation index based on RES. Hurtado and Pereria (2009) point out that for induction of fragmentation for the first 45 m of caving in the Diablo Regimiento mine, hydraulic fracturing method has been used as preconditioning of rock mass. So, for the fragmentation index ranking in Table 13, the fragmentation index of Diablo Regimiento (55), is chosen as the borders of medium fragmentation and good fragmentation potential.

## 6 Conclusions

A new method based on the RES and MICMAC was developed to assess the rock mass fragmentation, considering the indirect effect of all influencing parameters on each other as

well as the whole system. 23 parameters in 4 divided groups were recognized as the factors, which play the major roles in controlling the rock mass fragmentation. The direct interaction matrix corresponding to these parameters was constructed based on RES, then the indirect interaction matrix of influencing factors was obtained based on the MICMAC approach. The indirect Cause, Effect, and Interaction intensity bar chart indicated that the draw rate and discontinuity roughness have, respectively, the highest and lowest significant influence on fragmentation. The scaled relative interactive intensity along with the coefficient weight of all parameters was used to develop a fragmentation index.

The fragmentation indexes at the ReNo Mine, diablo Regimiento Mine, and Kemess Mine were reported to be 58.76, 49.54, and 59.88%. As seen, the Kemess Mine has the highest fragmentation potential while the Diablo Mine has the lowest fragmentation potential, in complying with the real data of the respective mines. It is noteworthy to mention that the amounts of the fragmentation potential indexes were calculated considering an average point for the multiple draw interaction, the height of air gap and the broken ore density.

The geomechanical and environmental parameters are generally uncontrollable so that only through some

**Table 11** Calculation of fragmentation index for case studies in both direct and indirect methods

parameters	$P_i$	$P_1$	$P_2$	$P_3$	$P_4$	$P_5$	$P_6$	$P_7$	$P_8$	$P_9$	$P_{10}$	$P_{11}$	$P_{12}$	$P_{13}$	$P_{14}$	$P_{15}$	$P_{16}$	$P_{17}$	$P_{18}$	$P_{19}$	$P_{20}$	$P_{21}$	$P_{22}$	$P_{23}$
Share of parameter (%)	$\frac{(C+E)_i}{\sum_{i=1}^n (C+E)_i}$	4.02	3.98	5.01	3.62	3.36	3.02	2.46	2.68	3.15	6.14	4.28	3.9	4.49	5.11	4.2	3.67	5.58	4.69	6.36	5.26	5.35	5.17	4.47
Normalized share of parameter	$\frac{1}{M_{P_{ij}}} \cdot \frac{(C+E)_i}{\sum_{i=1}^n (C+E)_i}$	1.01	1	1.25	0.91	0.84	0.76	0.62	0.67	0.79	1.54	1.07	0.98	1.12	1.28	1.05	0.92	1.4	1.17	1.59	1.32	1.34	1.29	1.12
Rating of $p_{ij}$ based on table 9	$p_{ij}$	0	4	3	2	2	4	1	0	1	4	3	3	0	2	2	1	3	3	4	4	4	2	4
Share of parameter in fragmentation index	$a_i * p_{ij}$	0	4	3.75	1.82	1.68	3.04	0.62	0	0.79	6.16	3.21	2.94	0	2.56	2.1	0.92	1.4	3.51	6.36	5.28	5.36	2.58	4.48
ReNo Fragmentation index	$Fgl_j = \sum_{i=1}^n a_i * p_{ij}$	66.66																						
Rating of $P_{ij}$ Based on table 9	$p_{ij}$	0	4	1	3	2	3	1	3	1	4	3	3	1	1	2	1	2	3	0	4	4	2	2
Share of parameter in fragmentation index	$a_i * p_{ij}$	0	4	1.25	2.73	1.68	2.82	0.62	2.01	0.79	6.16	3.21	2.94	1.12	1.28	2.1	0.92	1.4	3.51	6.36	5.28	5.36	2.58	2.24
Diablo Fragmentation index	$Fgl_j = \sum_{i=1}^n a_i * p_{ij}$	57.44																						
Rating of $P_{ij}$ Based on table 9	$p_{ij}$	0	2	2	3	4	3	2	3	0	3	3	4	4	1	2	4	1	3	2	4	4	2	4
Share of parameter in fragmentation index	$a_i * p_{ij}$	0.00	2.00	2.50	2.73	3.63	2.28	1.24	2.10	0.00	4.62	3.21	3.92	4.48	1.28	2.10	3.68	1.40	2.34	6.36	5.28	5.36	2.58	4.48
Kerness Fragmentation index	$Fgl_j = \sum_{i=1}^n a_i * p_{ij}$	67.78																						

**Table 12** Share of influence, effect, and interaction intensity in different groups

Group	Description											
	Influence intensity (%)				Effect intensity (%)				Interaction intensity (%)			
	Max	Min	Mean	Total of group	Max	Min	Mean	Total of group	Max	Min	Mean	Total of group
Geomechanical parameters	$(P_3)$ 7.55	$(P_7)$ 3.82	5.28	47.53	$(P_3)$ 2.26	$(P_7)$ 1	1.54	13.82	$(P_3)$ 5.01	$(P_7)$ 2.46	3.47	31.3
Environmental parameters	$(P_{10})$ 7.04	$(P_{14})$ 3.42	4.99	24.97	$(P_{14})$ 4.49	$(P_{11})$ 2.45	4.57	22.84	$(P_{10})$ 6.03	$(P_{12})$ 4.60	4.78	23.92
Geometrical parameters	$(P_{17})$ 3.91	$(P_{18})$ 2.94	3.40	13.61	$(P_{17})$ 11.45	$(P_{16})$ 6.33	5.76	23.04	$(P_{17})$ 7.98	$(P_{16})$ 4.81	4.54	18.14
Operational parameters	$(P_{19})$ 3.96	$(P_{22})$ 1.64	2.77	13.88	$(P_{22})$ 7.97	$(P_{23})$ 7.56	8.06	40.31	$(P_{19})$ 5.62	$(P_{22})$ 5.42	5.32	26.61

**Table 13** Ranking of fragmentation index

Class	Changes domain of fragmentation Index
Very good	$F_g I > 60$
Good	$60 > F_g I > 50$
Medium	$50 > F_g I > 40$
Bad	$50 > F_g I > 30$
Very bad	$30 > F_g I$

specific methods such as hydraulic fracturing and boundary weakening by vertical cuts (preconditioning of the rock mass), the parameters of these two groups can be controlled to optimize rock mass fragmentation. Given that fact the average shares of interaction for each parameter of the operational and geometrical groups are, respectively, 5.32% and 4.54%, higher than the average share of other groups, by making changes to the design and plan of production, and generally through changes in the geometrical

and operational parameters, the fragmentation potential of rock mass could be modified.

To determine the classification borders of the proposed index, more accurately, it is required that the hybrid RES method be applied to various caving mines, and after a comparison of the real data to those of the output in the hybrid RES model, the codification and ranking of the influencing parameters and fragmentation index would be gradually modified.

## References

- Ali KM, Hasan K (2002) Rock mass characterization to indicate slope instability in Bandarban: a rock engineering systems approach. *Environ Eng Geosci* 8(2):105–119
- Benardos AG, Kaliampakos DC (2004) Modelling TBM performance with artificial neural networks. *Tunn Undergr Space Technol* 19:597–605
- Brazovic A, Villaescusa E (2007) Rock mass characterization and assessment of block-forming geological discontinuities during caving of primary copper ore at the El Teniente mine, Chile. *Int J Rock Mech Mining Sci* 44:565–583
- Brown ET (2003) Block caving geomechanics. Julius Kruttschnitt Mineral Research Centre, Australia
- Catalan A, Rogers S, Elmo D, Webb G (2010). A DFN based approach to defining in situ, primary and secondary Fragmentation distributions for the Cadia East panel cave project. In: 2nd Int. Symp. On block and sublevel caving, Perth, pp 425–439
- Chung F, Simpson O (2018) Computing heat kernel pagerank and a local clustering algorithm. *Eur J Comb* 68:96–119
- Dershowitz WS, Lee G, Geie J, LaPointe PR (1998) FracMan: interactive discrete feature data analysis. Geometric modeling and exploration simulation. User Documentation
- Diaz R (2013) Indirect influence. *Adv Stud Contemp Math* 23:29–41
- Dorador L, Eberhardt E, Elmo D, Aguayo A (2014) Assessment of broken ore density variations in a block cave draw column as a function of fragment size distributions and fines migration. In: 3rd international symposium on block and sublevel caving, Santiago, Chile, pp 109–118
- Eadie B (2003) A framework for modeling fragmentation in block caving. Ph.D. Thesis, The University of Queensland
- Elmouttie MK, Poropat GV (2012) A method to estimate in situ block size distribution. *Rock Mech Rock Eng* 45:401–407
- Esterhuizen GS (2005) A program to predict block cave fragmentation. Technical report and user's guide
- Faramarzi F, Mansouri H, Farsangi MAE (2014) Development of rock engineering systems-based models for flyrock risk analysis and prediction of flyrock distance in surface blasting. *Rock Mech Rock Eng* 47(4):1291–1306
- Godet M (2000) The art of scenarios and strategic planning: tools and pitfalls. *Technol Forecast Soc Chang* 65(1):3–22
- Gomez R, Castro R, Casali A, Palma S, Hekmat A (2017) A comminution model for secondary fragmentation assessment for block caving. *Rock Mech Rock Eng* 50(11):3073–3084
- Hadjigeorgiou J, Lessard JF, Flament F (1995) Characterizing in situ block size distribution using stereological model. *Can Tunn J* 1:201–211
- Hudson JA (1992) Rock engineering systems: theory and practice. Ellis Horwood, Chichester
- Hudson JA (2013) A review of rock engineering systems (RES) applications over the last 20 years, rock characterization, modelling, and engineering design methods. Taylor and Francis Group, London
- Hudson JA, Harrison JP (2000) Engineering rock mechanics: an introduction to the principles. Elsevier, Oxford
- Hurtado JP, Pereria J (2009) Fragmentation back-analysis: sector Reservas Norte. Technical Report, Division El Teniente, Coldeco
- Hustrulid WA, Bullock RL (2001) Underground mining methods. Society for mining, metallurgy and exploration (SME), Englewood, pp 16–17
- Jakubec J, Lakaviev L, Major K (2016) Technical report for the kemess underground project and kemess east estimate. AuRico Metals Inc, Tornoto
- Jiao Y, Hudson JA (1995) The fully-coupled model for rock engineering systems. *Int J Rock Mech Min Sci Geomech Abstr* 32(5):491–512
- Jing L (2000) Block system construction for three-dimensional discrete element models of fractured rocks. *Int J Rock Mech Min Sci* 37:645–659
- Khalokakaie R, Zare NM (2012) The assessment of rock slope instability along the Khosh-Yeylagh main road (Iran) using a systems approach. *Environ Earth Sci* 67(3):665–682
- Kim T (2004) Development of a fuzzy logic based utilization predictor model for hard rock tunnel boring machines. Dissertation, Colorado School of Mines
- Latham JP, Lu P (1999) Development of an assessment system for the blast ability of rock masses. *Int J Rock Mech Min Sci* 36(1):41–55
- Laubscher DH (2000) A practical manual on block caving. Julius Kruttschnitt Mineral Research Centre, University of Queensland, Queensland
- Laubscher DH, Jakubec J (2000) The MRMR rock mass classification for jointed rock masses. Society of Mining Engineers, AIME, pp 475–481
- Lu J (2002) polyhedral rock blocks with arbitrary joints and faults. *Comput Geotech* 29:49–72
- Maerz NH, Germain P (1992) Block size determination around underground openings using simulations based on scanline mapping. In: Proceedings of the 2nd international conference on fractured and jointed rock masses. Lake Tahoe, CA, pp 34–41
- Mazzoccola DF, Hudson JA (1996) A comprehensive method of rock mass characterization for indicating natural slope instability. *Q J Eng Geol* 29:37–56
- Mohammad Khani M (2014) Application of rock engineering systems to block caving. Ph.D. Dissertation, School of Civil Engineering of the University of Queensland, Australia
- Noroozi M, Kakaie R, Jalali SE (2015) 3D stochastic rock fracture modeling related to strike-slip faults. *J Mining Environ* 6(2):169–181
- Pierce M (2010) A model for gravity flow of fragmented rock in block caving mines. Ph.D. Dissertation, Queensland University
- Rafie R, Ataei M, Khalokakaie R, Jalali SE, Sereshki F (2015) Determination and assessment of parameters influencing rock mass caveability in block caving mines using the probabilistic rock engineering system. *Int J Rock Mech Rock Eng* 48(3):1207–1220
- Rogers S, Elmo D, Webb G, Catalan A (2014) Volumetric fracture intensity measurement for improved rock mass characterisation and fragmentation assessment in block caving operations. *Rock Mech Rock Eng* 48(2):633–649
- Rozos D, Pyrgiotis L, Skias S, Tasagratos P (2008) An implementation of rock engineering system for ranking the instability potential of natural slopes in Greek territory. An application in Karditsa County. *Landslides* 5(3):261–270
- Sainsbury DP, Pierce ME (2011) A historical review of the development of numerical cave propagation simulations. In: Proceedings of the 2nd international FLAC/DEM symposium on numerical modelling, Melbourne



- Shin HS, Kwon YC, Jung YS, Bae GJ, Kim YY (2009) Methodology for quantitative hazard assessment for tunnel collapses based on case histories in Korea. *Int J Rock Mech Min Sci* 46(10):72–87
- Srikant A, Nicholas D, Rachmad L (2004) Visual estimation of fragment size distribution in the DOZ block cave. In: Proceedings of the 4th international conference and exhibition MassMin, Santiago, pp 286–290
- Villaescusa E, Brown ET (1992) Maximum likelihood estimation of joint size from trace length measurements. *Rock Mech Rock Eng* 25:67–87
- Vyazmensky A, Elmo D, Stead D, Rance J (2007) Combined finite-discrete element modeling of surface subsidence associated with block caving mining. In: Proceedings of 1st Canada-U.S. Rock Mechanics Symposium, Vancouver, pp 467–475
- Wang LG, Yamashita S, Sugimoto S, Pan C (2003) A methodology for predicting the in situ size and shape distribution of rock blocks. *Rock Mech Rock Eng* 36(2):121–142
- Zare NM, Jimenez R, Khalokakaie R, Jalali SE (2011) A probabilistic systems methodology to analyze the importance of factors affecting the stability of rock slopes. *Eng Geol* 118(3):82–92

**Publisher's Note** Springer Nature remains neutral with regard to jurisdictional claims in published maps and institutional affiliations.